Supplemental material

Ishii et al., https://doi.org/10.1085/jgp.201812243

Materials and methods

Preparation of cardiac β myosin

Cardiac β myosin was donated by Mr. Hwang Yongtae and Dr. Motoshi Kaya (University of Tokyo, Tokyo, Japan). It was extracted from fresh porcine ventricles as described previously (Harada et al., 1990; Schoffstall et al., 2006) in the laboratory of Dr. Hideo Higuchi (University of Tokyo). Porcine hearts were obtained at a local slaughterhouse.

Experimental system

In the experiments using cardiac β myosin, we used an inverted microscope IX73 (Olympus) with an objective lens (APON 60×OTIRF/1.49; Olympus), a mirror unit (U-FGWA; Olympus), an IR-LEGO unit (SIGMAKOKI), and an IR laser beam (KPS-STD-BT-RFL-1455-05-CO; Keopsys). The IR laser was irradiated for 10 s. Fluorescence images were recorded with an electron-multiplying charge-coupled device camera (iXon3; Andor Technology) at 10 frames per second. Experiments were carried out at 24°C ± 1°C.

Results and discussion

Use of recombinant Tm in the in vitro motility assay

The only chemical difference between recombinant and native Tm is that the first methionine is not acetylated in the recombinant protein (Hitchcock-DeGregori and Heald, 1987). Indeed, the affinity of unacetylated Tm (N-terminal methionine) for actin is reportedly lower than that of acetylated Tm (Heald and Hitchcock-DeGregori, 1988). In order to resolve this issue, Monteiro et al. (1994) attached Ala-Ser to the N terminus of recombinant Tm and successfully restored all functional properties known to depend on the acetylation of the initial methionine present in Tm (e.g., binding to actin; see Monteiro et al., 1994). Later, Schoffstall et al. (2006) used Gly (a nonpolar side chain) instead of Ala (as in the present study) and yielded similar results in the in vitro motility assay (Schoffstall et al., 2006). Therefore, the recombinant Tm with Gly-Ser attached to its N terminus is likely to produce functions similar to those of native Tm, at least in the in vitro motility assay.

Effects of heating on sliding movements of F-actin or reconstituted thin filaments with cardiac β myosin

We investigated whether or not IR laser irradiation accelerates the sliding movements of F-actin or reconstituted thin filaments (F-actin plus αTm–Tn) at pCa 9 and 5 on the porcine ventricular myosin-coated glass (Figs. S3 and S4).

First, we confirmed that at pCa 9 (+ATP), the sliding velocity of F-actin was rapidly increased upon laser irradiation (Fig. S3 A and Video 3). As with rabbit fast skeletal HMM (Video 1), the heating effect was more pronounced near the heat source, with the sliding velocity increasing as a function of temperature up to ∼40°C (i.e., ∼0.6 and ∼8.1 µm/s at 24°C and ∼40°C, respectively; Fig. S3 C). The observed velocity was similar to that previously reported by others using the same proteins (i.e., rabbit fast skeletal F-actin and porcine ventricular myosin; Malmqvist et al., 2004).

Laser irradiation induced sliding movements of reconstituted thin filaments at ∼36–38°C and above, up to ∼40°C even in the absence of Ca (pCa 9, +ATP); the sliding velocities were 2.1 and 2.2 µm/s at ∼36°C and ∼38°C; i.e., ∼20%, as compared with the maximal velocity of 8.1 µm/s at ∼40°C for F-actin (cf. ∼40% with fast skeletal HMM; see Fig. 3 C). These findings are consistent with the notion that mammalian cardiac thin filaments are partially activated under the relaxing condition at body temperature (see text), but to a lesser magnitude with cardiac β myosin as compared to when fast skeletal HMM was used. The apparently greater inhibitory effect of Tm–Tn on the sliding movements of reconstituted thin filaments with cardiac β myosin may be due to its slow attachment rate (hence a lesser fraction of actomyosin interaction) compared with fast skeletal myosin (cf. Walklate et al., 2016). The Q_{10} values were 5.0 and 4.4 for F-actin and reconstituted thin filaments at pCa 9, respectively (Fig. S3 D). A greater value of Q_{10} for F-actin as compared to that for the fast skeletal HMM (i.e., 2.4; Fig. 3 C) suggests a relatively high temperature sensitivity of f or g, or both in Huxley's model for cardiac myosin (see text).

We then investigated the effects of laser irradiation on F-actin or reconstituted thin filaments at pCa 5 (+ATP). Laser irradiation increased the sliding velocity for both F-actin and reconstituted thin filaments, of which effects were more pronounced near the heat source (Fig. S4 A and Video 4). At 24°C, the sliding velocity was slightly faster for reconstituted thin filaments (0.58 ± 0.02 and 1.19 ± 0.05 µm/s [$P < 0.001$] for F-actin and reconstituted thin filaments, respectively; Fig. S4 C). The Q_{10} values were 4.7 and 3.5 for F-actin and reconstituted thin filaments, respectively. Compared with the findings at pCa 9, while Q_{10} was similar to that for F-actin, it was

smaller for reconstituted thin filaments, and both were qualitatively similar to the results with fast skeletal HMM (cf. Figs. 3 D and 4 D). On the one hand, therefore, the on–off equilibrium of the thin filament state is shifted toward the on state at pCa 5, and therefore, the effect of heating-induced partial dissociation of Tm–Tn from F-actin is limited, resulting in a lesser magnitude of temperature dependence. On the other hand, the equilibrium is almost at the off state due to the fully suppressed actomyosin interaction by Tm–Tn at pCa 9, and therefore, the heating-induced partial dissociation of Tm–Tn will promote the attachment of a large fraction of myosin to thin filaments and the subsequent cross-bridge cycling (see text for details).

Interestingly, the sliding velocity was faster for reconstituted thin filaments than for F-actin at body temperature and above (e.g., 6.8 and 7.6 µm/s at ∼36 and ∼38°C, respectively), by ∼20–30%. One possible mechanism for this is that the cooperativity of cardiac thin filaments is more pronounced by cardiac myosin than by fast skeletal HMM, due to its longer duration of attachment to F-actin (cf. Walklate et al., 2016), resulting in enhanced recruitment of myosin attachment.

In order to fully uncover the molecular mechanisms of Ca^{2+}-independent thermal activation of myocardium (Oyama et al., 2012), future studies are warranted to investigate the effects of varying levels of heating on sliding movements of thin filaments at various pCa values using F-actin, Tm, Tn, and myosin that have been purified from fresh cardiac muscles of various animal species.

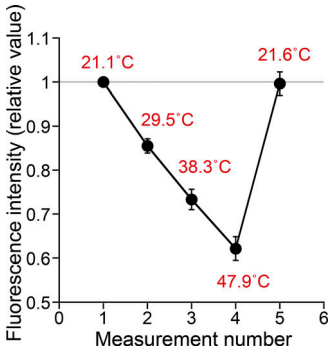

Figure S1. **Temperature dependence of the FI of rhodamine-phalloidin measured by a spectrophotometer.** Temperature-dependent changes in FI of rhodamine-phalloidin (0.2 µM in relaxing solution with no ATP or BSA) are shown. The temperature was increased from 21.1 ± 0.3°C to 47.9 ± 0.3°C and then decreased to return to the preheating level (21.6 ± 0.1°C). The x axis indicates the order of temperature measurement, and the y axis indicates FI normalized by the first measurement. Number of measurements, 3. Data represent mean ± SEM.

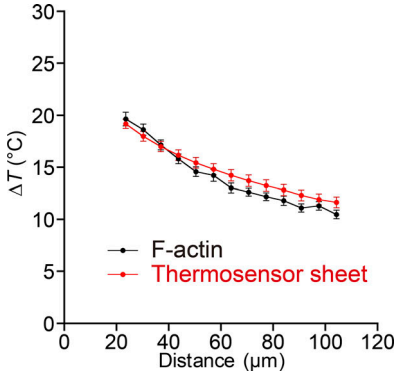

Figure S2. **Comparison of temperatures at various distances from the heat source measured by rhodamine-phalloidin–labeled F-actin and a fluorescent thermosensor sheet.** FIs at distances of ∼20–100 µm from the heat source were continuously measured to estimate temperatures by using two different methods under a fluorescence microscope. Δ*T* indicates the magnitude of the increase in temperature from the baseline temperature of 25°C. Black circles indicate data from rhodamine-phalloidin–labeled F-actin, and red circles incidate those from a thermosensor sheet. Note that similar values of Δ*T* were obtained at various distances. Because temperature was measured in solution on a glass-base dish, the data were not the same as those in Fig. 1 E (where temperature was measured in solution on a coverslip for the in vitro motility assay; see text). Number of measurements, 3. Data represent mean ± SEM.

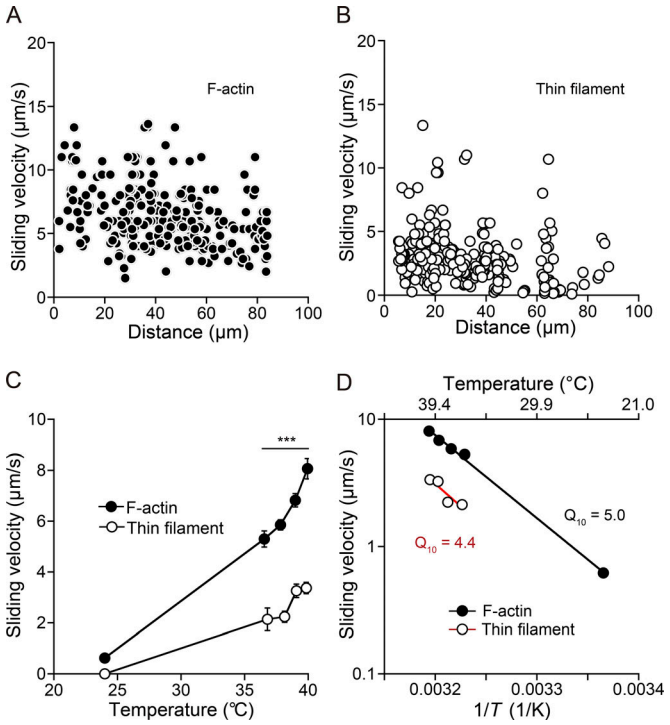

Figure S3. **Temperature dependence of sliding velocity of F-actin and reconstituted thin filaments with cardiac myosin at pCa 9. (A)** Relationship between the distance from the heat source and sliding velocity for F-actin. **(B)** Same as in A for reconstituted thin filaments. **(C)** Sliding velocity plotted against temperature. Closed circles, F-actin; open circles, reconstituted thin filaments. Sliding velocities were compared at 24°C (baseline temperature) and at higher temperatures raised by IR laser irradiation. Data indicate mean ± SEM for both the x and y axes. Sliding velocities at 24°C were 0.62 ± 0.02 μm/s (n = 253) and ∼0 μm/s for F-actin and reconstituted thin filaments, respectively. Those at higher temperatures were as follows: 5.30 ± 0.31 (n = 42) and 2.14 ± 0.44 μm/s (n = 32) at 36.55 ± 0.06 and 36.79 ± 0.05°C, 5.86 ± 0.20 (n = 93) and 2.24 ± 0.22 (n = 39) μm/s at 37.82 ± 0.04 and 38.15 ± 0.04°C, 6.82 ± 0.26 (n = 94) and 3.26 ± 0.26 μm/s (n = 75) at 38.99 ± 0.03 and 39.08 ± 0.04°C, and 8.07 ± 0.03 (n = 37) and 3.37 ± 0.22 μm/s (n = 82) at 39.94 ± 0.03 and 39.85 ± 0.02°C for F-actin and reconstituted thin filaments, respectively. ***, $P < 0.001$ for the y axis between groups (no significant differences were present on the x axis for each comparison). **(D)** Arrhenius plot of sliding velocity for F-actin and reconstituted thin filaments. T, absolute temperature. Average values in C were used. Sliding velocity (V) and temperature were expressed in logarithm. F-actin: $V = \exp(50.0 - 15{,}009/T)$ (R = 0.99). Reconstituted thin filaments: $V = \exp(53.1 - 16{,}243/T)$ (R = 0.92). Closed circles with a black solid line, F-actin; open circles with a red solid line, reconstituted thin filaments. Q_{10}, 5.0 (24–40°C) and 4.4 (37–40°C) for F-actin and reconstituted thin filaments, respectively.

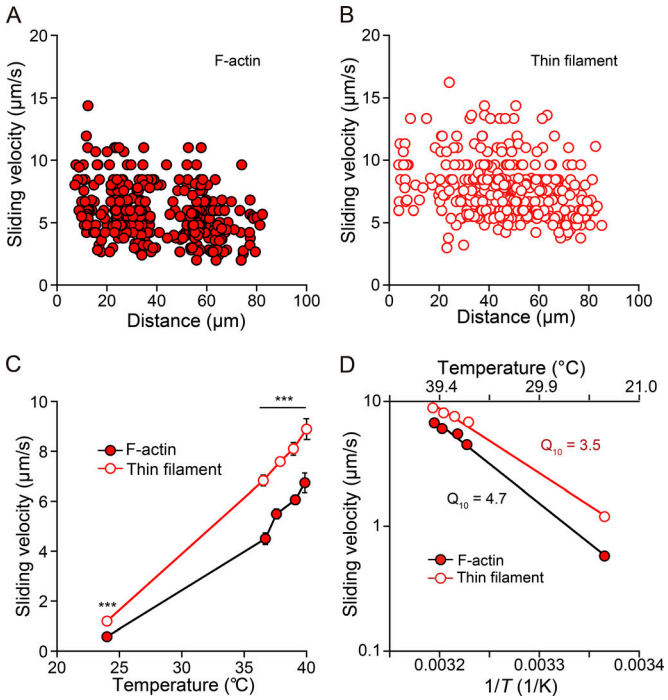

Figure S4. **Temperature dependence of sliding velocity of F-actin and reconstituted thin filaments with cardiac myosin at pCa 5. (A)** Relationship between the distance from the heat source and sliding velocity for F-actin. **(B)** Same as in A for reconstituted thin filaments. **(C)** Sliding velocity plotted against temperature. Closed circles, F-actin; open circles, reconstituted thin filaments. Sliding velocities were compared at 24°C (baseline temperature) and at higher temperatures raised by IR laser irradiation. Data indicate mean ± SEM for both the x and y axes. Sliding velocities at 24°C were 0.58 ± 0.02 (n = 201) and 1.19 ± 0.05 μm/s (n = 259) for F-actin and reconstituted thin filaments, respectively. Those at higher temperatures were as follows: 4.50 ± 0.23 (n = 54) and 6.83 ± 0.21 μm/s (n = 89) at 36.70 ± 0.05 and 36.53 ± 0.04°C, 5.50 ± 0.20 (n = 95) and 7.59 ± 0.16 μm/s (n = 156) at 37.59 ± 0.03 and 37.89 ± 0.03°C, 6.06 ± 0.18 (n = 130) and 8.10 ± 0.25 μm/s (n = 96) at 39.10 ± 0.02 and 38.95 ± 0.03°C, and 6.74 ± 0.39 (n = 44) and 8.89 ± 0.42 μm/s (n = 25) at 39.86 ± 0.02 and 40.01 ± 0.04°C for F-actin and reconstituted thin filaments, respectively. ***, P < 0.001 for the y axis between groups (no significant differences were present on the x axis for each comparison). **(D)** Arrhenius plot of sliding velocity for F-actin and reconstituted thin filaments. T, absolute temperature. Average values in C were used. Sliding velocity (V) and temperature were expressed in logarithm. F-actin: $V = \exp(48.7 - 14{,}624/T)$ (R = 0.99). Reconstituted thin filaments: $V = \exp(40.4 - 11{,}947/T)$ (R = 0.99). Closed circles with a black solid line, F-actin; open circles with a red solid line, reconstituted thin filaments. Q_{10} (24–40°C), 4.7 and 3.5 for F-actin and reconstituted thin filaments, respectively.

Table S1. **Comparison of amino acid sequences of proteins used in the present study and those of corresponding human cardiac proteins**

	Protein used in this study (NCBI sequence ID)	**Human cardiac protein (NCBI sequence ID)**	**Identity (%)**
Actin	Rabbit skeletal ACTA1 (XP_002722940.1)	Human cardiac ACTC1 (NP_005150.1)	372/377 (99%)
TnC	Bovine TNNC1 (NP_001029523.1)	Human TNNC1 (NP_003271.1)	160/161 (99%)
TnI	Bovine TNNI3 (NP_001035607.1)	Human TNNI3 (NP_000354.4)	195/212 (92%)
TnT	Bovine TNNT1 (XP_024831822.1)	Human TNNT2 (NP_000355.2)	217/229 (95%)
Myosin	Rabbit skeletal MYH2 (XP_008268946.1)	Human cardiac MYH7 (NP_000248.2)	1,586/1,938 (82%)
	Porcine cardiac MYH7 (NP_999020.2)	Human cardiac MYH7 (NP_000248.2)	1,890/1,935 (98%)

Identities were determined with Basic Local Alignment Search Tool (https://blast.ncbi.nlm.nih.gov/Blast.cgi). NCBI, National Center for Biotechnology Information.

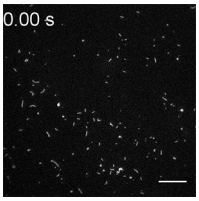

Video 1. **Thermal activation of F-actin at pCa 9.** Fluorescence images of F-actin on a rabbit fast skeletal HMM-coated coverslip were obtained. The IR laser was irradiated for 2 s, as indicated by "Heating." Baseline temperature, 25 ± 1°C. Objective lens, 60× (numerical aperture [N/A], 1.45; oil immersion). Speed, 33 frames per second (fps). Scale bar, 20 µm. See Fig. 2.

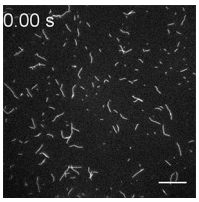

Video 2. **Thermal activation of reconstituted thin filaments at pCa 9.** Fluorescence images of reconstituted thin filaments on a rabbit fast skeletal HMM-coated coverslip were obtained. The IR laser was irradiated for 2 s, as indicated by "Heating." Baseline temperature, 25 ± 1°C. Objective lens, 60× (N/A, 1.45; oil immersion). Speed, 33 fps. Scale bar, 20 µm. See Fig. 2.

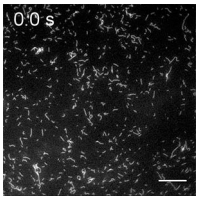

Video 3. **Thermal activation of F-actin with cardiac myosin at pCa 9.** Fluorescence images of F-actin on a porcine ventricular myosin-coated coverslip were obtained. The IR laser was irradiated for 10 s, as indicated by "Heating." Baseline temperature, 24 ± 1°C. Objective lens, 60× (N/A, 1.49; oil immersion). Speed, 10 fps. Scale bar, 20 µm. See Fig. S3.

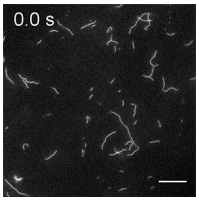

Video 4. **Thermal activation of reconstituted thin filaments with cardiac myosin at pCa 9.** Fluorescence images of reconstituted thin filaments on a porcine ventricular myosin-coated coverslip were obtained. The IR laser was irradiated for 10 s, as indicated by "Heating." Baseline temperature, 24 ± 1°C. Objective lens, 60× (N/A, 1.49; oil immersion). Speed, 10 fps. Scale bar, 20 µm. See Fig. S3.

References

Harada, Y., K. Sakurada, T. Aoki, D.D. Thomas, and T. Yanagida. 1990. Mechanochemical coupling in actomyosin energy transduction studied by in vitro movement assay. *J. Mol. Biol.* 216:49–68. https://doi.org/10.1016/S0022-2836(05)80060-9

Heald, R.W., and S.E. Hitchcock-DeGregori. 1988. The structure of the amino terminus of tropomyosin is critical for binding to actin in the absence and presence of troponin. *J. Biol. Chem.* 263:5254–5259.

Hitchcock-DeGregori, S.E., and R.W. Heald. 1987. Altered actin and troponin binding of amino-terminal variants of chicken striated muscle α-tropomyosin expressed in Escherichia coli. *J. Biol. Chem.* 262:9730–9735.

Malmqvist, U.P., A. Aronshtam, and S. Lowey. 2004. Cardiac myosin isoforms from different species have unique enzymatic and mechanical properties. *Biochemistry.* 43:15058–15065. https://doi.org/10.1021/bi0495329

Monteiro, P.B., R.C. Lataro, J.A. Ferro, and Fde.C. Reinach. 1994. Functional α-tropomyosin produced in Escherichia coli. A dipeptide extension can substitute the amino-terminal acetyl group. *J. Biol. Chem.* 269:10461–10466.

Oyama, K., A. Mizuno, S.A. Shintani, H. Itoh, T. Serizawa, N. Fukuda, M. Suzuki, and S. Ishiwata. 2012. Microscopic heat pulses induce contraction of cardiomyocytes without calcium transients. *Biochem. Biophys. Res. Commun.* 417:607–612. https://doi.org/10.1016/j.bbrc.2011.12.015

Schoffstall, B., A. Clark, and P.B. Chase. 2006. Positive inotropic effects of low dATP/ATP ratios on mechanics and kinetics of porcine cardiac muscle. *Biophys. J.* 91:2216–2226. https://doi.org/10.1529/biophysj.105.079061

Walklate, J., Z. Ujfalusi, and M.A. Geeves. 2016. Myosin isoforms and the mechanochemical cross-bridge cycle. *J. Exp. Biol.* 219:168–174. https://doi.org/10.1242/jeb.124594